CONFERENCE PROCEEDINGS, JANUARY 2025
Published by the Faculty of Science (FSC), FULafia
Print ISSN: 2354–3388 Online ISSN: 2315–7275 DOI: https://doi.org/10.62050/fscp2024.504

Single Oscillator Analysis, Electronic Polarizability and Optoelectronic Properties of Spin Coated Cobalt Doped Zinc Oxide Thin Films

M. B. Ochang[1]✉, A. T. Adepoju[1], P. R. Jubu[1], N. J. Tsaviv[2], E. V. Tikyaa[3], B. J. Akeredolu[4], F. Aungwa[1], E. Tersoo[1] & Y. Yusof[5,6]

[1]Department of Industrial Physics, Joseph Sarwuan Tarka University, Makurdi, Nigeria
[2]Department of Chemistry, Joseph Sarwuan Tarka University, Makurdi, Nigeria
[3]Department of Physics, Joseph Sarwuan Tarka University, Makurdi, Nigeria
[4]Department of Physics, Federal University Wukari, Nigeria
[5]Nano Optoelectronic Research (NOR) and Technology Lab., School of Physics, Universiti Sains Malaysia, 11800 USM Penang
[6]School of Physics, Universiti Sains Malaysia, 11800 USM Penang
✉bikomchang@yahoo.co.uk/

Abstract: The structural, optical, single oscillator analysis, electronic polarizability, and optoelectronic properties of Co:ZnO thin films prepared via sol-gel spin coating are reported. X-ray diffraction analysis revealed a hexagonal wurtzite crystal structure, with crystallite size increasing from 15.9 (0 mol%) to 16.37 nm at 4 mol.% then decreased to 14.86 nm at 8 mol%, attributed to lattice distortion and micro-strain. Strain energy density increased with Co doping, reflecting enhanced lattice distortions. UV-vis spectroscopy reveals a decrease in the optical band gap from 3.72 eV for 0 mol% to 2.76 eV for 8 mol%, while the refractive index increased from 2.23 to 2.4. The oscillator energy in the single oscillator analysis through the Wemple-DiDomenico model increases from 4.091 eV (0 mol%) to 6.909 eV (8 mol%), the dispersive energy rises from 1.156 to 38.154 eV, and the oscillator strength increases from 0.36×10^{-5} to 29.8×10^{-5}. Electronic polarizability also increased from 2.26×10^{-25} to 2.45×10^{-25} cm³, thus reflecting increased polarization arising from structural and electronic changes. Optoelectronic properties such as the charge carrier, concentration plasma frequency, relaxation time and optical mobility were also maximized at 6 mol% cobalt doping and decreased at 8 mol%. On the other hand, the optical resistivity decreased from 9.49×10^{-21} to 2.29×10^{-22} Ωm. These findings therefore reveal that Co doping enhances the optical and electronic properties of ZnO thin films, hence making them suitable for optoelectronic applications, including sensors, solar cells, and nonlinear optical devices.

Keywords: oscillator- energy, dispersive- energy, electronic polarizability, optoelectronic

Introduction

Zinc oxide (ZnO) is an abundant, inexpensive, and environmentally friendly direct wide band gap (3.37 eV) II–IV compound semiconductor that finds extensive application in diodes [1], biomedical [2], gas sensors [3], optoelectronics [4], photocatalysis [5], piezoelectric device [6], and transparent conducting oxides [7]. In recent times, ZnO have been doped with transition metals such as cobalt (Co) [8], manganese (Mn) [9], iron (Fe) [10], nickel (Ni) [11], and others introduce new energy states within the ZnO band gap, leading to enhanced or novel functionalities suitable for various technological applications. However, the substitution of Zn^{2+} ions by Co^{2+} ions in the ZnO lattice is stable and suitable as the ionic radii difference of Zn^{2+} (0.74 Å) and Co^{2+} (0.75 Å) is within the limit of Hume-Rothery rule. Recently Co doped ZnO thin films have been fabricated using sol-gel spin coating [12, 13], pulse laser deposition [14, 15], sputtering [16, 17], atomic layer deposition [19] and others. In this study, pure ZnO and Co-doped ZnO thin films were produced using sol-gel spin coating deposition technique. This method was chosen because of its advantages such as Simplicity and cost-effectiveness, good control over composition and doping concentration and Suitability for large-area coatings.

It is observed that, the single oscillator analysis and the electronic polarizability of cobalt doped zinc oxide thin films is rarely sighted in the literature. Single oscillator analysis is a powerful technique for characterizing the optical properties of materials (Co:ZnO thin films inclusive). It provides valuable insights into the material's electronic structure, dispersion parameters (oscillator energy, dispersive energy and oscillation strength) [20, 21, 22], and the effects of doping and annealing. These insights are crucial for optimizing the material's performance in various applications, making single oscillator analysis an essential tool in the study and development of Co:ZnO thin films. Electronic polarizability is a critical factor influencing the optical, dielectric, electrical, nonlinear optical, and magnetic properties of materials [23, 24, 25]. Understanding and controlling this property can lead to enhanced performance in various applications such as optoelectronics, spintronics, sensors, and nonlinear optical devices. The interplay between the polarizability and other material properties enables the tailoring of Co:ZnO thin films for specific technological applications.

In this paper, we report the single oscillator analysis and electronic polarizability of cobalt doped zinc oxide thin films synthesized by sol-gel deposition technique. The Wemple-Didomenico (WDD) model was used to

determine single oscillator parameters such as oscillator energy, dispersive energy, oscillator strength and static refractive index. Furthermore, the electronic polarizability was evaluated using UV-Vis spectroscopy data. Moreover, the effect of cobalt concentration on the oscillator parameters and electronic polarizability of Co:ZnO was investigated. The insights provided by this study are crucial for optimizing the material's performance in various applications such as optoelectronics, spintronics, sensors, and nonlinear optical devices.

Materials and Methods

Synthesis of Co:ZnO thin films

Preparation of precursor solutions

The analytical grade reagents of zinc acetate dehydrate ($(CH_3COO)_2Zn.2H_2O$), Cobalt acetate tetra hydrate ($C_4H_{14}CoO_8$), methanol (CH_3OH) and triethanolamine (TEA) were used in the preparation of the precursor solutions. Firstly, 0.4 M of zinc acetate dehydrate was dissolved in the mixture of methanol and triethanolamine (TEA) solution at room temperature. The molar ratio of TEA to Zinc acetate dehydrates was kept at 1:1. In the same way, 0.4M of dopant source, cobalt acetate tetra hydrate was prepared with methanol as solvent. The dopant concentrations were 0, 4.0, 6.0 and 8.0 wt%. The solutions were stirred at 50^{o}C for 20 min using a water bath stirrer (WBS-6pro, Joan lab). The resultant solutions were aged at room temperature for 24 h to form gel.

Deposition of Co: ZnO thin films

The sol gel spin coating deposition technique was used in the fabrication of the Co:ZnO thin films.

Prior to the deposition, the soda-lime glass (SLG) substrates were cut into 2.5 by 2.5 cm sizes. The SLG substrates were washed with detergent, rinsed with de-ionized water, cleaned with ethanol and then rinsed again with de-ionized water. The washed SLG substrates were then dried in a laboratory oven (model TT 9053, Techmmel & Techmmel, USA) at 100^{o}C for 15 min. The ZnO and the Co:ZnO thin films were coated on the SLG substrates using the vacuum spin coater (VTC-100, Shenyang Kejing Auto-Instruments Co Ltd, China). The precursor solution (gel) was dropped on the SLG substrate and spun at 2500 rpm for 20 seconds. After this, the film was baked in the laboratory oven at 180^{o}C for 10 minutes and allowed to cool to room temperature. The coating process was repeated 10 times for each sample. The deposited films were annealed at 400^{o}C for one hour in a model SXL muffle furnace (Gallenkomp, England).

Characterization of the Co:ZnO thin films

The optical and structural properties of the synthesized Co:ZnO thin films were measured using the JENWAY Spectrophotometer (Cole palmer Ltd, UK), X-ray Diffractometer (XRD) D8 Advanced BRUKER .The thickness of the film was measured by the Stylus profilometer VEECO Dektak150.

Results and Discussion

Structural properties of Co:ZnO thin films

The X-ray diffraction (XRD) pattern of undoped and Co-doped ZnO thin films at different concentrations of cobalt ion (Fig. 1). The XRD pattern corresponds with diffraction standard card number 36-1451 and revealed that, the the Co:ZnO thin films are polycrystalline and exhibit hexagonal wurtzite crystal structure [26]. Moreover, no extra peak ascribed to Co dopant was detected. This suggests that the films are of a single phase [27]. The pure ZnO thin film showed preferred orientation in the 1 0 1 direction and that as the cobalt content increased, the peak intensities were observed to decrease gradually. This suggest a decline in crystallinity caused by incorporation of Co^{2+} into the Zn^{2+} ion lattice sites of the ZnO matrix [27].

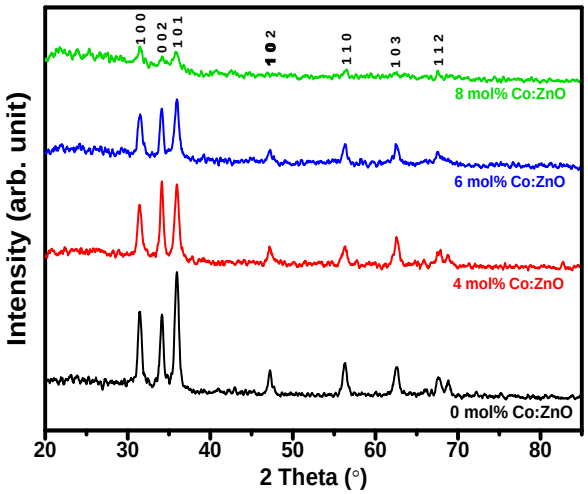

Figure 1: X-ray diffraction pattern for Co:ZnO thin films

The average crystallite size D, of the Co:ZnO films was calculated using the Sherrer's formula Eq.1 [28].

$$D = \frac{0.9\lambda}{\beta cos\theta} \quad (1)$$

Where β is the full width at half maximum (FWHM) at Bragg's angle θ, for the dominant peaks of (100), (002) and (101) planes. While λ is the wavelength of the x-ray (λ=1.5406 Å). The lattice parameters a and c, were estimated from the Eq.2 and Eq.3 [29].

$$a = \frac{\lambda}{\sqrt{3} sin\theta_{(100)}} \quad (2)$$

$$c = \frac{\lambda}{sin\theta_{(002)}} \quad (3)$$

The unit cell volume V_u, the crystallite volume V_c, and the number of unit cells in a crystallite N_u, were determined by using Eq.4, Eq.5, Eq.6 [26], and then presented in Table 1.

$$V_u = \frac{\sqrt{3}a^2 c}{2} \quad (4)$$

$$V_c = D^3 \quad (5)$$

$$N_u = \frac{V_c}{V_u} \quad (6)$$

Table 1: Structural properties of cobalt doped zinc oxide thin films

Co Conc. mol%	2θ (deg.)			*FWHM β(Radian)*			*Lattice Parameters (Å)*		v x10^{-2} (nm)^3	V x10^3 (nm)^3	Nu x10^4	Average Crystallite Size D (nm)	Dislocation density δ x 10^{1}m^{-2}	Micro-strain ε x 10^{-3}
	100	002	101	100	002	101	a	c						
0	31.5	34.20	35.90	0.0088	0.0085	0.0120	3.27	5.239	4.87	4.05	8.31	15.94	4.24	7.94
4	31.4	34.15	35.90	0.0108	0.0750	0.0102	3.29	5.247	4.91	4.39	8.94	16.37	4.02	7.83
6	31.4	34.10	35.90	0.0110	0.0081	0.0102	3.29	5.254	4.92	3.28	6.67	14.86	4.98	8.65
8	31.4	34.10	35.95	0.0119	0.0100	0.0090	3.29	5.254	4.92	3.40	6.92	15.04	4.62	8.50

The crystallite size for the undoped ZnO is found to be 15.94 nm, but between 4 mol% and 8 mol% of Co-doped ZnO, the crystallite size decreased from 16.37 to 14. 86 nm. This decrease in crystallite size can be attributed to increased micro-strain and lattice distortion caused by the incorporation of larger Co^{2+} ion (ionic radius ~0.75 Å) into the smaller Zn^{2+} ion (ionic radius = 0.74 Å) site in the ZnO lattice [30]. This can also be due to enhancement of nucleation sites [31], which also inhibits crystal growth. The variation of unit cell volume, crystallite volume and number of unit cells with cobalt concentration in Co:ZnO is presented in Fig. 2. It is observed that, the unit cell volume of Co-doped ZnO thin films increases with cobalt content primarily due to the substitution of Zn^{2+} ions with larger Co^{2+} ions in the ZnO lattice. This substitution causes the lattice to expand slightly, resulting in an increased unit cell volume. Additionally, any lattice distortion introduced by the cobalt ions can also contribute to this volume expansion [32]. Also noteworthy is the fact that, the number of unit cell volumes decreased with increase in Co content. This can be due to increased dislocations to due to Co doping (as seen in Table 1). These defects can result in a higher packing density or increased grain boundary area, which in turn reduces the number of unit cells that can be formed within Co:ZnO lattice [32].

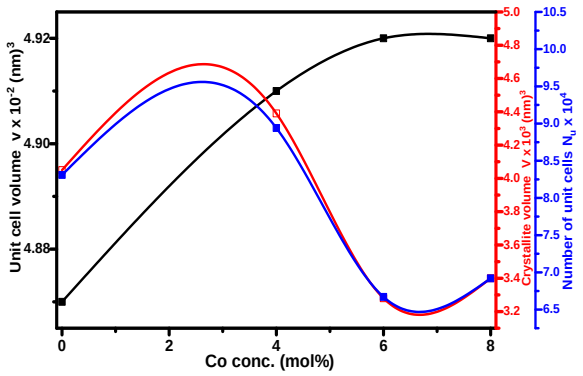

Figure 2: Variation of unit cell volume, crystallite volume and number of unit cells with cobalt concentration in Co:ZnO thin films

Bond length

The bond length refers to the distance between the atoms in a crystal lattice. When ZnO is doped with cobalt, the introduction of Co ions can alter the Zn-O bond length as the dopant Co ionic radius is larger compared to the host Zn ion.

The bond length L of the Co:ZnO thin films is calculated using Eq.7 [31].

$$L^2 = \frac{a^2}{3} + \left(\frac{1}{2} - u\right)^2 c^2 \qquad (7)$$

Where a and c are the lattice constants and *u*, the positional parameter. The positional parameter for the hexagonal wurtzite structure is obtained from the relation Eq.8:

$$u = \left(\frac{a^2}{3c^2} + 0.25\right) \qquad (8)$$

The calculated values of the bond lengths for the pure ZnO and the Co-doped ZnO thin films are presented in Table 1). This difference can be due to the presence of oxygen vacancies induced by Co^{2+} due to their low formation energy in the ZnO lattice [33]. The variation of bond length and crystallite size at different Co doping level is presented in Fig. 3. It is observed that, the bond length in the Co:ZnO thin films increases with Co content in the ZnO lattice. The increase in bond length can be ascribed to the incorporation of Co^{2+} with larger ionic radius into Zn^{2+} ion site with smaller ionic radius. An increase in bond length typically introduces strain into the crystal lattice. Bond length induced strain can impede the growth of large crystallites, leading to smaller crystallite sizes [34, 35]. This is consistent with the crystallite size as shown in Fig. 3 where bond length is inversely proportional to crystallite size.

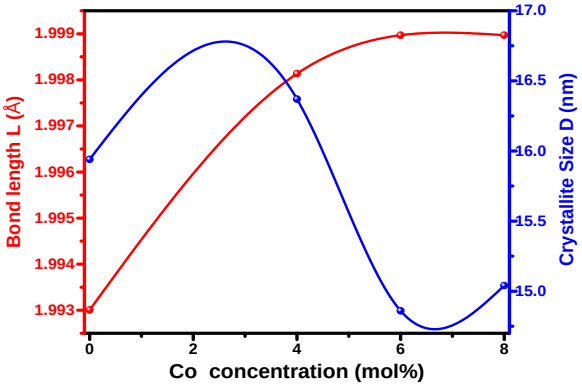

Figure 3: Effect of cobalt concentration on crystallite size and bond length of Co:ZnO thin films

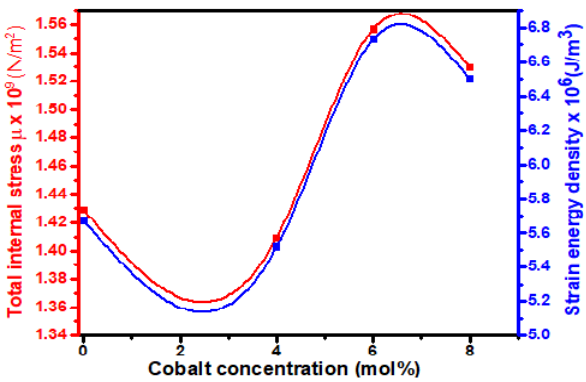

Figure 4: Variation of total internal stress and strain energy density with Co concentration in Co:ZnO thin films

Strain energy density

The strain energy density is a measure of the elastic energy stored per unit volume due to deformation. The strain energy density in Co-doped ZnO thin films is influenced by the strain, which arises from lattice mismatch or doping-induced lattice distortions. It is given by the Eq. 9 [36].

$$E_d = \frac{1}{2} E \varepsilon^2 \quad (9)$$

It is observed that, the strain energy density is directly proportional to the total internal stress as seen in Fig. 4.

Optical properties

Optical absorption and transmission of cobalt doped ZnO thin films

The absorption spectrum (Fig. 5a) indicates that increasing cobalt concentration caused a red-shift in the absorption edge. Generally, for Co:ZnO thin films, absorption occurs in the UV-visible region, typically between 300 nm and 700 nm. The shift in absorption edge can be attributed to due to defect states and the sp-d exchange interactions [37].

The transmission spectra (Fig. 5b) show a decrease in transmittance as Co concentration increased from 4 mol% to 8 mol%. This is an expected behaviour, as transition metal doping creates additional absorption centers that reduce transparency of the thin films. In the pure ZnO thin film, the transmittance in the visible region typically exceeds 80% [38]. With Co doping, the transmission can dropped from about 70%–50%. This result is consistent with reports of [39].

Absorption and extinction coefficients of Co:ZnO thin films

The absorption coefficient (α) describes how strongly a material absorbs light at a specific wavelength. It is related to the direct or indirect band gap transitions in the material. The absorption coefficient is determined from Eq. 10 [28].

$$\alpha = \frac{2.303A}{d} \quad (10)$$

Where, A is the absorbance and d, the thickness of the film. Fig. 5c shows the absorption coefficient of cobalt doped zinc oxide thin films. It is noted that, in ZnO, the absorption coefficient is typically in the range of 10^4 to 10^5 cm^{-1} in the UV-visible region [39]. The introduction of Co into ZnO modifies the absorption behaviour due to the creation of additional defect states and possible band gap narrowing [37]. Higher Co concentrations often lead to increased absorption in the visible region due to d–d transitions of Co^{2+} ions [40].

The extinction coefficient (k) measures the material's ability to absorb light and dissipate energy as heat. It is related to the absorption coefficient by the Eq.11

$$k = \frac{\alpha\lambda}{4\pi} \quad (11)$$

Where λ is the wavelength. Fig. 5d depicts extinction coefficient as a function of photon energy for the Co:ZnO thin films. It is observed that, a high k value in the UV range suggests strong electronic transitions, while an increased k in the visible region indicates additional defect states or mid-gap absorption centres caused by Co doping [41]. More so, in pure ZnO, k is generally low (< 0.1) in the visible region but increases at high photon energy (above 3.10 eV) due to fundamental absorption [39]. Co doping often leads to an increase in k at longer wavelengths, suggesting enhanced defect-related absorption.

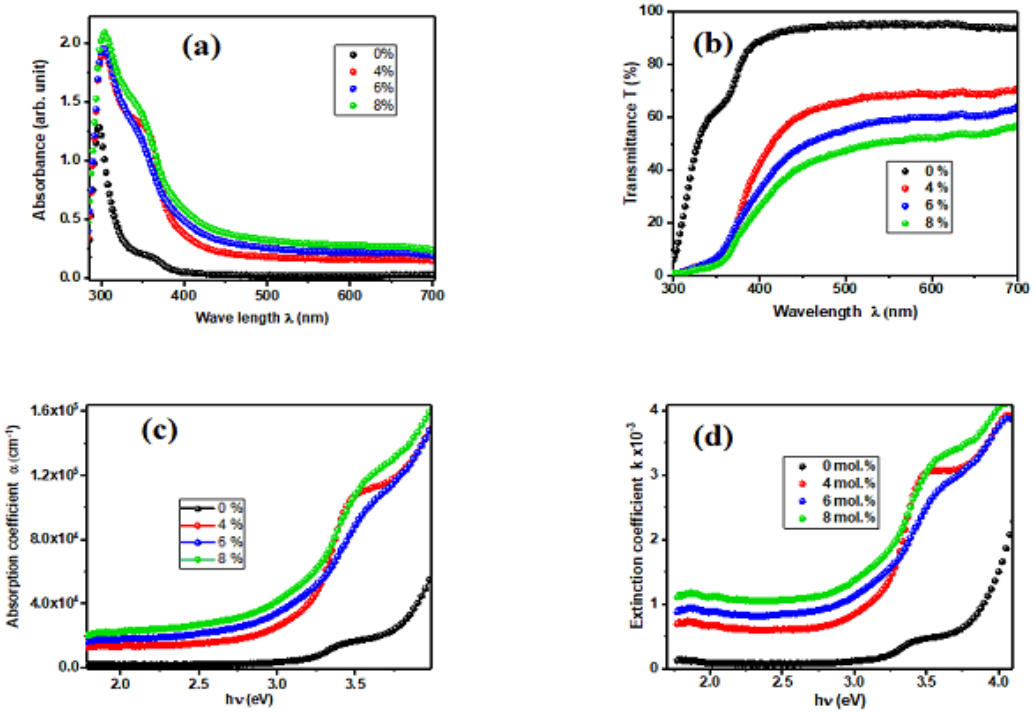

Figure 5: (a) Absorbance (b) Transmission (c) Absorption Coefficient and (d) Extinction coefficient of Co:ZnO thin films

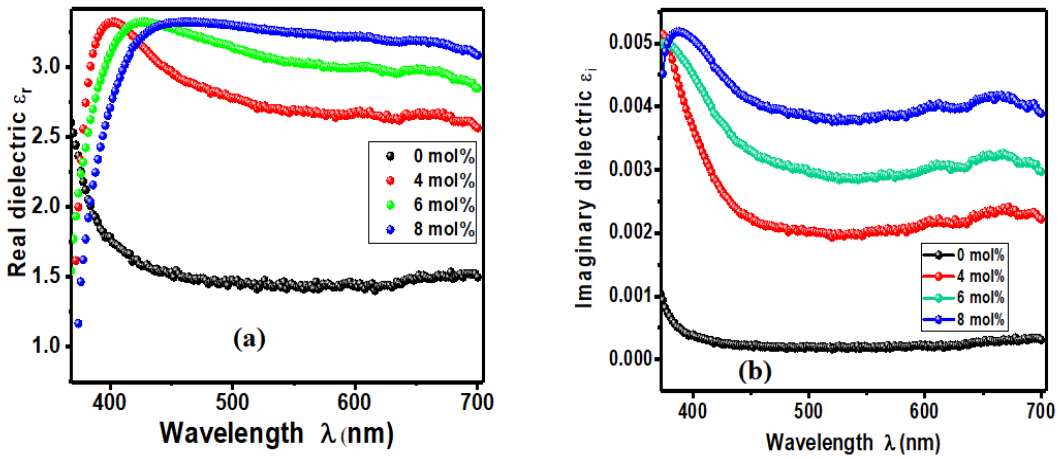

Figure 6: (a) Real dielectric constant and (b) Imaginary dielectric constant Co:ZnO thin films

Dielectric properties of cobalt doped zinc oxide thin film

Dielectric constant is a crucial property of semiconductor material. There are two components of dielectric constants namely: the real dielectric constant (ε_r) and the imaginary dielectric constant (ε_i). The real dielectric constant measures how much a semiconductor will impede the speed of light without absorbing energy. Whereas, imaginary dielectric constant is a measure of how much a material absorbs energy from a time varying field. The dielectric constants are given by Eqs. 12 and 13.

$$\varepsilon_r = n^2 - k^2 \quad (12)$$

$$\varepsilon_i = 2nk \quad (13)$$

Where n and k are refractive index and extinction coefficient, respectively

Figure 6(a-b) depict the real and imaginary dielectric properties of Co:ZnO thin films prepared by sol gel spin coating method

The variation of real part of the real dielectric constant ε_1 with Co doping in ZnO thin films follows distinct trends. At low Co concentration, a slight rise in dielectric constant is observed. This can be due to the introduction of localized states in the optical band gap, which enhance the Co:ZnO's polarization ability [41]. Higher ε_i values at moderate Co doping levels suggest improved optical performance, making Co:ZnO films suitable for optoelectronic applications.

It is noticeable that, pure ZnO has lower imaginary dielectric constant due to fewer mid-gap states. As Co doping increases in ZnO thin films, the imaginary dielectric constant generally shows a variation which can be attributed to increase in optical absorption [42], changes in free carrier concentration [41] and localized defect states [43].

Optical band gap refractive Index and Urbach energy

The Tauc's relation in Eq.14 was used to obtain the optical band gap energy values of the Co:ZnO thin films.

$$\alpha h\nu = Y\left(h\nu - E_g\right)^n \quad (14)$$

Where, α is the absorption coefficient, $h\nu$ is the incident photon energy, E_g is optical band gap, Y is a constant and n is a factor which depends on the allowed electronic transition. $n = \frac{1}{2}$an d $n = 2$ for direct and indirect allowed transitions, respectively. Therefore,

$$(\alpha h\nu)^2 = Y\left(h\nu - E_g\right) \quad (15)$$

To determine the optical band gap energy, the variation of $(\alpha h\nu)^2$ with respect to photon energy $h\nu$ is plotted for the thin films under study as shown in Fig. 7. The value of the band gap is obtained by extrapolating the linear portion of the curve from on the horizontal axis $(h\nu = 0)$. The determined values of the optical band gap of the Co:ZnO thin films are presented in Table 3. It is observed that, the optical band gap decreases with increasing Co concentration, from 3.72 eV at 0 mol% to 2.76 eV at 8 mol%. This reduction suggests that cobalt doping introduces localized states near the conduction band, narrowing the band gap, which can be attributed to sp-d exchange interactions between the band electrons and the localized d-electrons of Co ions [44].

In terms of the optical band gap, the refractive index in calculated from Dimitrov and Sakka's relation Eq.16:

$$\frac{n^2-1}{n^2+2} = 1 - \sqrt{\frac{E_g}{20}} \quad (16)$$

The calculated values of the refractive index as presented in Table 2, increased slightly as Co concentration in ZnO lattice rises, from 2.23 at 0 mol% to 2.47 at 8 mol%. This behaviour indicates increased densification and changes in the electronic environment, which are common in doped materials.

Table 2: Optical properties of Co:ZnO thin films

Co conc. mol.%	optical bandgap E_g (eV)	Refractive index η	Urbach energy E_u (meV)
0	3.72	2.23	197
4	3.12	2.37	417
6	2.88	2.43	891
8	2.76	2.47	822

Urbach energy (E_u) is the width of the tail of localized defect states in the band gap. These defect states trap the excited electrons, thereby preventing direct transition of electrons from valence to the conduction band. It is responsible for the absorption tail which extends into the forbidden gap. This absorption tail is called the Urbach tail and is related with the Urbach energy. The Urbach energy is calculated using Eq. 17a.

$$\alpha = \alpha_0 exp \frac{h\nu}{E_u} \quad (17a)$$

Where α is the absorption coefficient, $h\nu$ is the photon energy, E_u the Urbach energy and α_0 a constant. Eq.17a can be transformed into a linear equation as in Eq. 17b.

$$\ln \alpha = \ln \alpha_0 + \frac{h\nu}{E_u} \quad (17b)$$

The Urbach energy is obtained from the reciprocal of the slope of the linear fitting of the plot of $\ln \alpha$ vs $h\nu$ (Fig. 8 (b). The determined Urbach energy values are presented in Table 3. It can be seen that, the Urbach energy, representing the disorder in the thin films, rises significantly from 197 meV at 0 mol% to 891 meV at 6 mol%, then decreases slightly to 822 meV at 8 mol%. This trend highlights that Co doping initially increases structural disorder due to ion incorporation but might stabilize at higher concentrations [45].

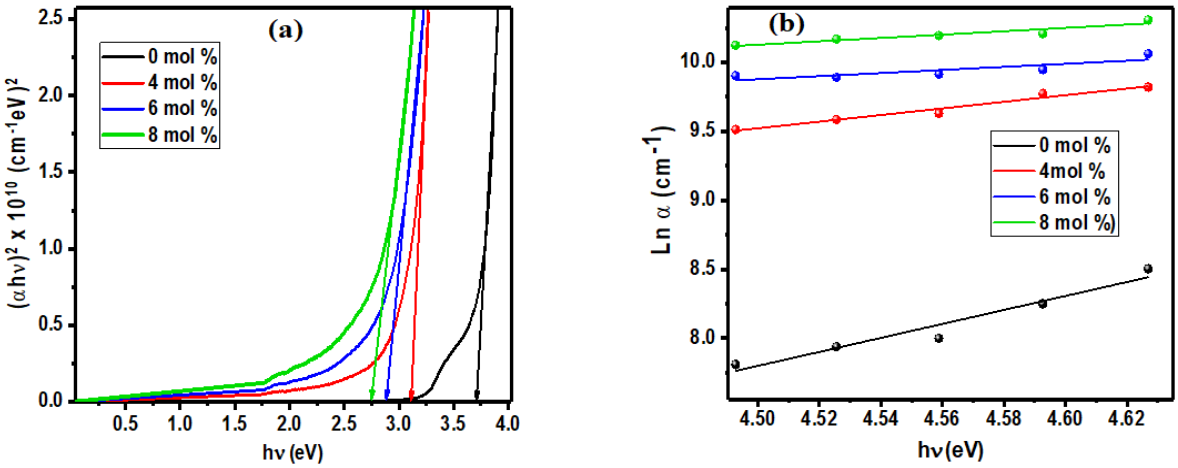

Figure 7: (a) Tauc's Plots and (b) Ln α versus hν plots for Co: ZnO thin films

Single oscillator analysis cobalt doped zinc oxide thin film

The single oscillator analysis of the Co:ZnO thin films was carried out using the Wemple-DiDomenico (WDD) single oscillator model (Eq.18) to determine parameters such as oscillator energy, dispersive energy, oscillator strength and static refractive index. The WDD model shows refractive index as function of photon energy below the inter-band absorption edge [36].

$$n^2_{(h\nu)} = 1 + \frac{E_d E_0}{{E_0}^2 - (h\nu)^2} \quad (18)$$

Where E_d is the dispersive energy, E_o is single oscillator energy and $n_{h\nu}$ is wavelength dependent refractive index expressed in Eq. 19 [47, 48].

$$n_{(\lambda)} = \frac{1+\sqrt{R}}{1-\sqrt{R}} \quad (19)$$

The dispersion energy E_d, measures the average strength of inter band optical transitions and depends onmaterial's electronic structure. The oscillator energy (E_0) represents the average energy of optical transitions and is a measure of the material's electronic resonance. It is associated with optical direct band gap of the semiconductor material.

The E_d and E_o for the Co:ZnO thin films were determined from the linear fitting of the plots of $(n^2-1)^{-1}$ versus $(h\nu)^2$ of Fig. 11(a). $\frac{E_0}{E_d}$ is the intercept on the vertical axis while $\frac{1}{E_o E_d}$ is the slope of the linear fitted curve.

The static refractive index (zero frequency refractive index) n_0 from dispersion parameters was obtained using Eq.20.

$$n_0 = \sqrt{1 + \frac{E_d}{E_o}} \quad (20)$$

The optical moments provide insight into the material's electronic structure, revealing information about the density and distribution of energy states when it interacts with electromagnetic waves (lights).There are two optical moments namely first (M_{-1}) and third (M_{-3}) optical moments. The first moment indicates the Co:ZnO's polarizability, providing information on the ease with which electrons in the Co:ZnO thin films can be displaced by an external electric field. Higher values of M_{-1} imply that the Co:ZnO can respond more strongly to low-energy electromagnetic fields which is often desirable for enhancing light absorption.

The first and third optical moments are given by Eq.21 and Eq.22, respectively [49].

$$M_{-1} = \frac{E_d}{{E_o}^2} \quad (21)$$

The third optical moment,

$$M_{-3} = \frac{E_d}{{E_0}^4} \quad (22)$$

Where, Ed is the dispersive energy and Eo is the oscillator energy

The oscillator strength S_o and the average oscillator wavelength λ_o of the CZO thin films were determined by using the Sellmeier equation (Eq.23) [28].

$$(n^2-1)^{-1} = \frac{1}{S_o\,\lambda_0{}^2} - \frac{1}{S_o\lambda^2} \qquad (23)$$

The linear fitting of the plots of $(n^2-1)^{-1}$ versus λ^{-2} (Fig. 11b) for all the films were employed to calculate oscillator strength S_o and the average oscillator wavelength λ_o. The slope of the fitted line equals $\frac{1}{S_o}$ and the intercept on the vertical axis equals $\frac{1}{S_o\,\lambda_0{}^2}$.

The calculated values of the dispersion energy E_d , the effective oscillation energyE_o, the static refractive indexn_0, optical moments (M_{-1}) and (M_{-3}), oscillator strength and wavelength of the Co:ZnO thin films with different Co concentrations are reported in Table 4.

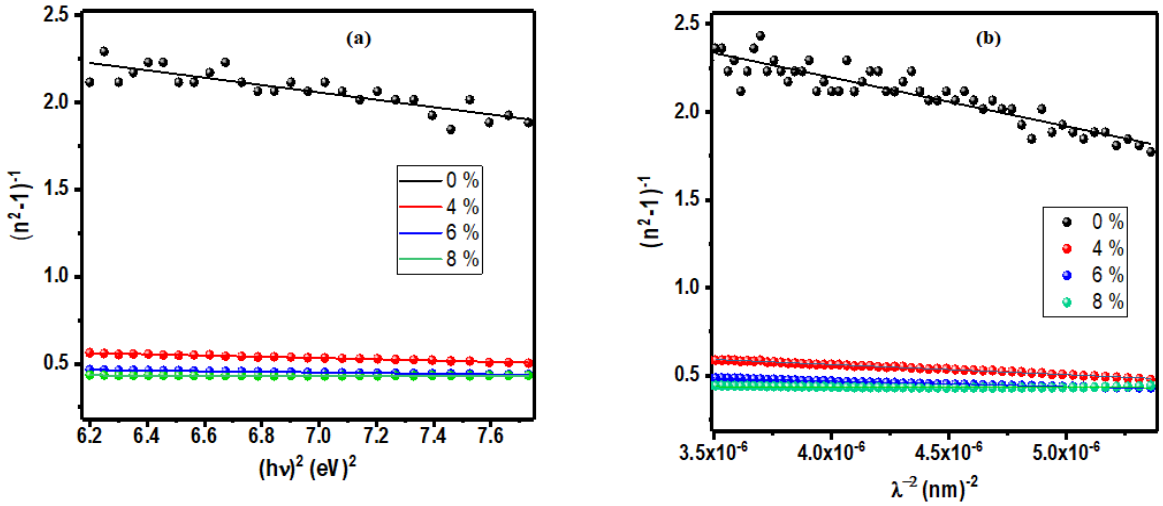

Figure 8: (a) Wemple-Didomenico plots for CZO thin films, (b) Sellmeier plots for CZO thin film

Table 3: Refractive index dispersive parameters of cobalt doped zinc oxide thin films

Co Conc. (Mol.%)	Optical band gap E_g (eV)	Dispersive energy E_d (eV)	Oscillator Energy E_0 (eV)	Static refractive Index n_o	E_o/E_g	M_{-1}	M^{-3}	S_ox 10^{-5}	λ_o (nm)
0	3.72	1.156	4.091	1.133	1.10	0.283	0.211	0.36	958.66
4	3.12	5.929	4.662	1.507	1.49	1.272	0.036	1.73	214.25
6	2.88	9.688	5.610	1.651	1.99	1.727	0.018	3.23	135.49
8	2.76	38.154	6.909	1.8045	2.50	2.256	0.002	29.8	38.84

Results depict that Ed increases significantly from 1.156 eV to 38.154 eV as the Co ion concentration rose from 0 to 8 mol%**.** This in dispersive energy suggests that Co ions significantly strengthen the interaction between light and the Co:ZnO thin film, thereby increasing the films' refractive and absorptive capacities [50]. The observed result makes Co-doped ZnO thin films particularly suitable for applications requiring high refractivity, such as coatings, waveguides, and optical devices. Also, the E_o increased with Co concentration, from 4.091 eV at 0 mol% to 6.909 eV at 8 mol%**.** The Oscillator energy of thin film is empirically associated with the lowest band gap by the relationship, E_o=2.5 E_g [51]. The increase in E_0 predicts that cobalt doping shifts electronic transitions to higher energy levels. This is associated with the modification of ZnO's electronic structure due to the incorporation of Co ions, enables the energy required for inter band transitions [44]. An increase in the E_0 improves the Co:ZO optical energy storage and resonance capabilities, making it suitable in optoelectronic applications like filters and resonators that require stable, high-energy optical properties.

Furthermore, the oscillator strength S_0, increased appreciably, from 0.36 × 10^{-5} at 0 mol% to 29.8 × 10^{-5} at 8 mol%. The significant increase in the S_0 depicts that Co-doped ZnO thin films are highly effective in absorbing and emitting light, making them ideal for photovoltaic devices, lasers, and light-emitting diodes (LEDs).

Electronic polarizability

Electronic polarizability (α_e) measures the material's ability to polarize under an applied electric field, which depends on its electronic structure.

Electronic polarizability of the CZO can be obtained using the Clausius-Mosotti model of the local field polarization Eq. 24.

$$\alpha_e = \frac{3}{4\pi N_A}\left(\frac{n^2-1}{n^2+2}\right)V_m \qquad (24)$$

Where n, is the refractive index of the thin film, N_A, is the Avogadro's number (6.02 x 10^{23}) and V_m , is the molecular volume obtained from

$$V_m = \frac{M}{\rho} \qquad (25)$$

Where M and ρ is the Molar mass and density respectively of bulk CZO material

The calculated electronic polarizability of the CZO and its variation owith Co concentration in ZnO lattice is presented in Table 4. It is noted that, α_e increases steadily with Co concentration, from 2.26×10^{-25} cm³ at 0 mol% to 2.45×10^{-25} cm³ at 8 mol%.

This result revealed that, the polarizability is enhanced by the incorporatio of Co ions into the ZnO lattice. This can be attributed to creation of greater electronic cloud distortion under an applied electric field due to Co doping in ZnO matrix [44] Also, the replacement of Zn^{2+} with Co^{2+}, which has a different electronic structure, increased the dielectric polarizability of the ZnO lattice [49]. The increase in polarizability can be attributed to electronic structure modification [45], lattice distortion [51] and charge carrier concentration [49].

Metallization criterion and linear optical susceptibility

The metallization criterion (M) is a parameter that evaluates the potential of a material to transition from an insulating to a metallic state. It provides insight into the electronic structure and bonding characteristics of the material. It is calculated based on the refractive index n, as shown in Eq.26

$$M = 1 - \left(\frac{n^2-1}{n^2+2}\right) \qquad (26)$$

The calculated values of M are presented in Table 4. It is observed that, M decreases from 0.430 at 0 mol% Co to 0.370 at 8 mol% Co**.** This decline suggests that as cobalt concentration increases, the material exhibits a stronger tendency toward metallic behaviour. The decreasing M value corresponds to the narrowing of the optical band gap, which indicates that the energy required for electron excitation decreases due to the incorporation of Co ions which consequently created defect states and enhanced electron-lattice interactions [44].

Linear optical susceptibility (χ) is a quantity that defines the material's response to an external optical field. It determines material's ability to polarize under light. It is determined as shown in Eq.27 [27].

$$\chi = \frac{\varepsilon-1}{4\pi} \qquad (27)$$

Where, ε is dielectric constant

The calculated values of χ as shown in Table 4 increases from 0.316 at 0 mol% Co to 0.406 at 8 mol% Co. The increase in the linear optical susceptibility depicts enhanced polarizability of the films under study. As Co ions are incorporated into the ZnO matrix, the electronic density in the material is enhanced. This structural modification improves the Co:ZnO's nonlinear optical properties [51]. The increase in χ of the Co:ZnO thin films improves the material's optical interactions, making it suitable for applications in optoelectronic devices, such as waveguides, optical modulators, and lasers.

Table 4: Electronic polarizability metallicity and optical susceptibility of cobalt doped Zinc oxide Thin films

Co conc. mol.%	Metallization Criterion M	Electronic Polarizability α_e x10^{-25}	Optical dielectric Constant ε_{opt}	Linear Optical Susceptibility χ
0	0.430	2.26	3.973	0.316
4	0.394	2.41	4.617	0.367
6	0.380	2.46	4.905	0.390
8	0.370	2.45	5.101	0.406

Optoelectronic properties of co-doped ZnO thin films

Density of states (DOS)

The density of states (DOS) reflects the number of available electronic states per unit volume at a specific energy.The optoelectronic properties such as density of states and free charge carrier concentration (N) can be obtained from the Spitzer-Fan Model (SFM) as given in Eq.28 [28].

$$\varepsilon_r = \varepsilon_\infty - \frac{1}{4\pi^2\epsilon_0}\left(\frac{e^2}{c^2}\right)\left(\frac{N}{m^*}\right)\lambda^2 \qquad (28)$$

where $\frac{N}{m^*}$ density of states), ε_r is the real dielectric constant, ε_∞ high frequency dielectric constant , e is the electronic charge, c speed of light, N, is charge carrier concentration and m^* is the effective mass (m^*= 0.18 m_e) [52]. Where, m_e is the electron mass and ϵ_0 is the permittivity in free space. The density of states $(\frac{N}{m^*})$ for all the samples of CZO thin films was determined from the linear fitting of the plot of ε_r on the vertical axis and λ^2 on the horizontal axis (Fig. 9a) where $\frac{1}{4\pi^2\epsilon_0}\left(\frac{e^2}{c^2}\right)\left(\frac{N}{m^*}\right)$ equals the slope and ε_∞ is the intercept on the vertical axis.

The computed values of DOS and free charge carrier concentration for different Co concentration in CZO thin films are reported in Table 6. Results indicate that DOS increases significantly, from 0.67×10^{39} at 0 mol% to 2.64×10^{39} at 6 mol%**,** before dropping to 1.09×10^{39} at 8 mol%. However, at 8 mol%, the decrease in DOS may be due to structural disorder [44].

Relaxation time

Relaxation time is a measure of the average time between charge carrier collisions. The relaxation time for the CZO thin films was determined using the Drude free electron which expresses the imaginary dielectric constant as a function of incident photon wavelength given in Eq.29 [53].

$$\varepsilon_i = \frac{1}{4\pi^3\epsilon_0}\left[\frac{e^2}{c^3}\right]\left[\frac{N}{m^*}\right]\left[\frac{1}{\tau}\right]\lambda^3 \qquad (29)$$

where the symbols have their usual meanings. The relaxation time is determined from the slope of the linear fitting of the plot of ε_i against λ^3 (Fig. 9b).

By knowing the ratio term N/m*, the electronic charge e, the electric permittivity of air ϵ0 and the speed of light c, the relaxation time τ was calculated. The calculated values of the relaxation time as reported in Table 5 showed that, τ increased from 3.56×10^{-4} s to

9.39×10^{-4} s as Co doping rose from 0 to 6 mol%, and then declined to 2.06×10^{-4} s at 8 mol% Co doping. The increase in relaxation time between 0 to 6 mol% ls indicates reduced scattering and enhanced carrier mobility while, the decline of relaxation time at 8 mol% suggests that excessive Co doping introduces more defects and scattering centers [45].

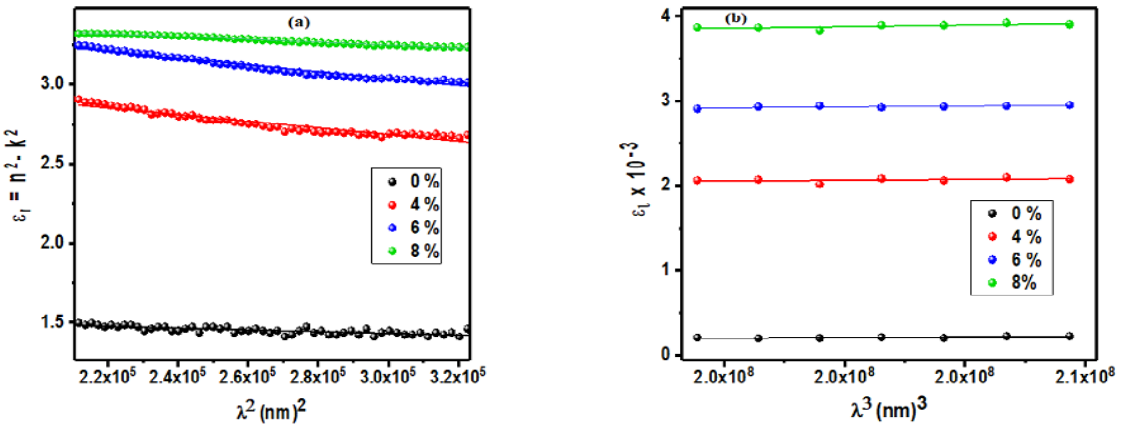

Figure 9: (a) Spitzer-Fan Plots and (b) Linear fitting of the plot of $\varepsilon_i$against λ^3 for CZO thin films

Table 5: Optoelectronic properties of cobalt doped Zinc oxide Thin films

Co conc. Mol.%	Density of states N/m x 10^{39}	Plasma frequency ω_p x10^{12} (Hz)	Charge carrier concentration N x10 ^{8}	Relaxation Time τ x10^{-4} (s)	Optical mobility μ_{opt} x10^{7}cm2/V·s	Optical resistivity ρ_{opt} (Ω.m)
0	0.67	1.93	1.70	3.56	3.12	9.49E-21
4	2.54	7.35	6.48	9.27	8.14	2.51E-22
6	2.64	7.64	6.73	9.39	8.25	2.29E-22
8	1.09	3.16	2.79	2.06	1.81	6.09E-21

Plasma frequency

Plasma frequency corresponds to the collective oscillation frequency of free charge carriers in the material. The plasma frequency (ω_p) of all free charge carriers involved in the optical transitions for the CZO thin films at different Co content was calculated using Eq.30 [54].

$$\omega_p = \frac{e^2 N/m^*}{\epsilon_0} \qquad 30$$

where e, electronic charge, ϵ_0 is the permittivity in free space $8.85\times 10^{-12}\ Fm^{-1}$, and N/m^* the DOS.

The result of the calculated plasma frequency for the various CZO thin films as presented in Table 5 indicated that that when the Co concentration rose from 0 ml% to 6 mol%, plasma frequency increased from 1.93×10^{12} Hz to 7.64×10^{12} Hz, and then declined to 3.16×10^{12} Hz at 8 mol% of Co doping. The increase in ωp at lower concentrations indicates a higher concentration of free carriers, which is ascribed to the level of Co doping. The drop at higher concentrations might be due to scattering effects or saturation of dopant-induced carriers [55]. Higher plasma frequency at moderate doping levels enhances the material's optical conductivity and transparency in certain spectral ranges, making it suitable for transparent conducting films and other optoelectronic applications.

Optical mobility and resistivity

The ease of carrier movement in an optical field is reflected in optical mobility. Conversely, optical resistivity quantifies how resistant a substance is to the movement of optical charge carriers. The Drude Free Electron Model was used to calculate the optical mobility (μ_{opt}) and resistivity (ρ_{opt}) of the CZO thin films under investigation using Eqs 31 and 32.

$$\mu_{opt} = \frac{e\tau}{m^*} \qquad (31)$$

$$\rho_{opt} = \frac{4\pi}{\tau\omega_p{}^2} \qquad (32)$$

Where, e is the electronic charge, $\tau$is the relaxation time m^* is the effective mass of charge carrier and ω_p is the plasma frequency

The calculated values of optical mobility and resistivity of the CZO thin films at different Co concentration are presented in Table 5. Results pointed out that, optical mobility increased from 3.12×10^7 cm²/V•s to 8.25×10^7 cm²/V•s as Co concentration increased from 0 to 6 mol%, and decreased to 1.81×10^7 cm²/V•s at 8 mol%. The rise in optical mobility at lower Co doping levels shows improved carrier transport, while the decrease at 8 mol% indicates reduction in mobility likely due to increased scattering [44]. Moreover, Enhanced optical mobility at optimal doping levels improves optoelectronic performance, ideal for high-speed optical communication systems. On the other hand, optical

resistivity ρopt, decreases sharply, from 9.49 × 10^{-21} Ω•m at 0 mol% to 2.29 × 10^{-22} Ω•m at 6 mol%, then rises to 6.09 × 10^{-21} Ω•m at 8 mol%. The decrease at lower doping levels corresponds to enhanced conductivity, while the rise at higher doping levels reflects increased carrier scattering and reduced charge transport [49]. The implication is that, low optical resistivity at moderate doping enhances the material's suitability for transparent conducting layers in displays and solar cells.

Conclusion

Co:ZnO thin films were successfully synthesized by sol gel spin coating deposition technique. The prepared films were characterized via X-ray diffraction (XRD) analysis and UV-vis spectroscopy to investigate the structural properties, single oscillator analysis, electronic polarizability, and optoelectronic properties of Co:ZnO thin films. XRD analysis revealed a hexagonal wurtzite crystal structure, with crystallite size increasing from 15.9 (0 mol%) to 16.37 nm at 4 mol.% then decreased to 14.86 nm at 8 mol%,. Strain energy density increased with Co doping, reflecting enhanced lattice distortions. UV-vis spectroscopy reveals a decrease in the optical band gap from 3.72 eV for 0 mol% to 2.76 eV for 8 mol%, while the refractive index increased from 2.23 to 2.47. The oscillator energy in the single oscillator analysis through the Wemple-DiDomenico model increases from 4.091 eV (0 mol%) to 6.909 eV (8 mol%), the dispersive energy rises from 1.156 to 38.154 eV, and the oscillator strength increases from 0.36 × 10^{-5} to 29.8 × 10^{-5}. Electronic polarizability also increased from 2.26 × 10^{-25} to 2.45 × 10^{-25} cm³, thus reflecting increased polarization arising from structural and electronic changes. The metallicity criterion and linear optical susceptibility were also evaluated. Optoelectronic properties like the charge carrier concentration, density of state, plasma frequency, relaxation time and optical mobility were also maximized at 6 mol% cobalt doping and decreased at 8 mol%. On the other hand, the optical resistivity decreased from 9.49 × 10^{-21} to 2.29 × 10^{-22} Ωm. These findings therefore reveal that Co doping enhances the optical and electronic properties of ZnO thin films, hence making them suitable for optoelectronic applications, including sensors, solar cells, and nonlinear optical devices.

Declaration of competing interest: The authors declare that they have no known competing financial interests or personal relationships that could have influenced the work reported in this article.

Acknowledgements: The authors wish to acknowledge the staff of Nano–physics Laboratory, Joseph Tarkaa University, Makurdi, Nigeria for providing the sol-gel spin coating unit and UV–Visible spectrophotometer equipment. The authors also appreciate the Nano Optoelectronic Research and Technology (NOR) Lab, School of Physics, Universiti Sains Malaysia, 11800 USM Penang for carrying out X-ray Diffraction of the samples understudy.

References

[1] Yakuphanoglu, F. (2011). Controlling of electrical and interface state density properties of ZnO:Co/p-silicon diode structures by compositional fraction of cobalt dopant *Microelectron. Reliab.*, 51, 2195–2199.

[2] Jiang, J., Pi, Q. & Xia, Y. (2021). ZnO-based nanostructures for biomedical applications. *Materials Today Advances*, 10, 100126.

[3] Sharma, R., Singh, P. & Sharma, A. (2022). ZnO-based gas sensors: A comprehensive review. *J. of Sensors and Sensor Syst.*, 11(2), 159-179.

[4] Cao, J., Zhang, Y., Wang, D. & Liu, X. (2022). Advances in ZnO-based light-emitting diodes: From material development to device engineering. *Advanced Optical Materials*, 10(5), 2102071.

[5] Foster, H. A., Ditta, I. B., Varghese, S. & Steele, A. (2021). Photocatalytic degradation of organic pollutants using ZnO nanostructures: A review. *Env. Sci.: Nano*, 8(3), 709-737.

[6] Park, J. H., Lee, M. & Kim, S. (2023). Flexible and wearable piezoelectric devices based on ZnO nanowires. *Nano Energy*, 97, 107153.

[7] Fortunato, E., Barquinha, P. & Martins, R. (2020). Oxide semiconductor thin-film transistors: A review of recent advances. *Advanced Materials*, 32(15), 1904424.

[8] Sharma, P., Gupta, S. K. & Singh, R. K. (2013). Optical and structural properties of Co-doped ZnO thin films. *Materials Chemistry and Physics*, 141(2-3), 367-372.

[9] Vishnu, C. V., Kumar, V. R. & Narayana, C. (2022). Tailoring the photoluminescence and magnetic properties of ZnO thin films by Mn doping. *Materials Today Communications*, 30, 103197.

[10] Goh, G. K. L., Zhang, X. & Liu, C. (2021). Structural and magnetic properties of Fe-doped ZnO thin films. *Journal of Alloys and Compounds*, 866, 158911.

[11] Bhowmik, A., Chattopadhyay, P. P. & Mandal, K. (2021). Influence of Ni doping on the structural, optical and electrical properties of ZnO thin films. *Journal of Materials Science: Materials in Electronics*, 32(5), 6734-6745.

[12] Xiao, Y., Li, J., Zhang, H. & Chen, S. (2021). Structural, optical, and magnetic properties of Co thin films prepared by sol-gel spin coating. *J. of Materials Sci.*, 56(15), 8756-8765.

13] Zhang, L., Wang, J., Li, H. & Chen, Y. (2020). Influence of annealing temperature on the properties of Co thin films. *Thin Solid Films*, 697, 137836.

[14] Kim, J., Lee, S., Park, H. & Choi, Y. (2022). Structural and magnetic properties of Co thin films produced by pulsed laser deposition. *Journal of Applied Physics*, 131(3), 033906.

[15] Lee, S., Kim, J., Park, H. & Choi, Y. (2021). Effects of laser influence on the properties of Co thin films deposited by pulsed laser deposition. *Applied Surface Science*, 547, 149064.

[16] Wang, H., Zhang, Y., Liu, X., Chen, L. & Zhao, J. (2023). Deposition of Co thin films by RF magnetron sputtering: Optimization of sputtering power and gas ratios. *Surface and Coatings Technology*, 433, 127142.

[17] Liu, Y., Zhang, X., Chen, L., Wang, J. & Li, Q. (2021). Magnetic and optical properties of Co thin films deposited by sputtering. *Journal of Magnetism and Magnetic Materials*, 529, 167939.

[18] Chen, X., Li, Y., Zhang, M. & Wang, J. (2022). Synthesis of Co thin films using metal-organic chemical vapor deposition. *Journal of Crystal Growth*, 584, 126612.

[19] Park, J., Lee, S., Kim, H. & Choi, Y. (2022). Atomic layer deposition of Co thin films for advanced electronic applications. *ACS Applied Materials & Interfaces*, 14(3), 3625-3633.

[20] Akazawa, M. (2020). Optical properties and single oscillator analysis of doped ZnO thin films. *J. of Applied Physics*, 128(4), 045302.

[21] Lee, J., Kim, H. & Lee, S. (2022). Single oscillator analysis of ZnO thin films: Effects of annealing temperature. *Materials Research Bulletin*, 150, 111772.

[22] Sahin, Y., Aksu, A. & Demir, U. (2021). Influence of Co doping on the optical properties of ZnO thin films: A single oscillator analysis. *Journal of Materials Science: Materials in Electronics*, 32(10), 13579-13588.

[23] Chen, Y. & Zhang, X. (2023). Electronic polarizability and dielectric properties of high-k materials: A comprehensive review. *Journal of Materials Science*, 58(7), 3456-3472.

[24] Li, H. & Wang, J. (2024). Tunable refractive index in photonic materials through controlled electronic polarizability. *Applied Physics Letters*, 122(4), 041102.

[25] Kim, D. & Lee, K. (2024). Polaronic contributions to electronic polarizability in transition metal oxides. *Physical Review B*, 100(2), 025202.

[26] Poongodi, G., Anandan, P., Kumar, R. Mohan, Jayavel, R. (2015). Studies on visible light photocatalytic and antibacterial activities of nanostructured cobalt doped ZnO thin films prepared by sol–gel spin coating method. *Spectrochimica Acta Part A: Molecular and Biomolecular Spectroscopy*, 148, 237–243. doi:10.1016/j.saa.2015.03.134

[27] Deepa Rani T., Sakshi Joshi A. & Leela S (2021). Studies on structural and optical properties of Cobalt doped ZnO thin films prepared by Sol-gel spin coating technique. *Materials Today: Proceedings* 43, 3166–3168.

[28] Ochang, M. B., Ahemen, I., Amah, A. N., Onoja, A. D. & Yusof, Y. (2023). Effect of Substrate Temperature on the Structural Optical and Electrical Properties of New $Cu_2Cd_{0.8}Mn_{0.2}SnS_4$ Photo-absorber Layer for Solar Cells, *Results in Optics*, doi: https://doi.org/10.1016/j.rio.2023.100509

[29] Xu, L, Xinghua, Z, Kangxin, J. & Dingyu, Y. (2020). Study on structural and optical properties of Mn-doped ZnO thin films by sol-gel method. *Optical Materials*, 100, 109657. https://doi.org/10.1016/j.optmat.2020.109657

[30] Dhruvashi, N. & Shishodia, P. K. (2016). Effect of Cobalt doping on ZnO thin films deposited by sol-gel method. *Thin Solid Films*, doi:10.1016/j.tsf.2016.05.028

[31] Lalit, K. G., Preeti, G., Gairola, S. P, Mohan, C. M., Promod, K., Sachin, K., Dushyant, K., Vivek, A., Aragon, F., Soler, A. G. & Swart, H. C. (2021). Cobalt doping induced shape transformation and its effect on luminescence in zinc oxide rod-like nanostructures. *Journal of Alloys and Compounds*, doi:10.1016/j.jallcom.2021.159189

[32] Mohaseb, M. A. (2023). Effect of Co doping onto physical properties of ZnO films and its UV detection performance. *J. Mater. Sci.: Mater. Electron.*, 34, 12-19. https://doi.org/10.1007/s10854-023-10633-1

[33] Zong, Y., Sun, S., Meng, Y., Wang, H., Xing, X., Li, X. Zheng (2019). Doping effect and oxygen defects boost room temperature ferromagnetism of Co-doped ZnO nanoparticles: experimental and theoretical studies. *RSC Adv.*, 9 23012–23020, https://doi.org/10.1039/c9ra03620b

[34] Amakali, Theopolina, Likius. S. Daniel, VeikkoUahengo, Nelson Y. Dzade & Nora H. de Leeuw (2020). Structural and optical properties of ZnO thin films prepared by molecular precursor and sol–gel methods. *Crystals*, 10(2), 132. https://doi.org/10.3390/cryst10020132

[35] Marinov, Georgi, BilianaGeorgieva, Marina Vasileva & Tsvetanka Babeva (2023). Study of structure, morphology and optical properties of cobalt-doped and Co/Al-co-Doped ZnO thin films deposited by electrospray method. *Applied Sciences*, 13(17), 9611. https://doi.org/10.3390/app13179611

[36] Alsaad, Ahmad M., Ahmad, Ahmad A., Al-Bataineh, Qais M., Bani-Salameh, Areen A., Abdullah, Hadeel S., Qattan, Issam A., Albataineh, Zaid M. & Telfah, Ahmad D. (2020). *Optical, Structural, and Crystal Defects Characterizations of Dip Synthesized (Fe-Ni) Co-Doped ZnO Thin Films. Materials, 13(7), 1737–*. doi:10.3390/ma13071737.

[37] Gupta, S. & Kumar, D. (2019). Optical properties of cobalt-doped ZnO thin films: A review. *Materials Research Bulletin*, 115, 102-110.

[38] Singh, R., Sharma, M. & Kumar, A. (2020). Structural and optical modifications in ZnO thin films due to cobalt doping. *Applied Surface Science*, 500, 144007.

[39] Sharma, P., Kumar, M. & Singh, R. (2018). Bandgap engineering in Co-doped ZnO thin films: Effects of concentration and annealing. *Optical Materials*, 75, 234-241.

[40] Pathak, T., Sharma, M. & Singh, R. (2021). Influence of transition metal doping on ZnO thin films' optical properties. *Journal of Materials Science*, 56(3), 1825-1837.

[41] Singh, P., Mehta, B. R. & Chauhan, S. (2021). Influence of cobalt doping on dielectric properties of ZnO thin films. *Journal of Applied Physics*, 129(5), 055303.

[42] Dar, M. A., Gul, R., Khan, M., Majid, K. & Qurashi, A. (2019). Optical and dielectric properties of transition metal-doped ZnO thin films. *Materials Res. Bull.*, 118, 110484.

[43] Dutta, A., Das, R., Paul, D. & Kar, S. (2018). Role of defect states in tuning the optical and dielectric properties of Co-doped ZnO thin films. *Materi. Chem. and Phy.*, 206, 241-250.

[44] Sharma, N., Verma, S., Gupta, R. & Patel, A. (2022). Analysis of polarizability and bandgap tailoring in ZnO films with Co doping. *Optical Materials*, *127*, 112245.

[45] Raj, A., et al. (2021). Doping effects on optical properties of ZnO thin films: A comprehensive study. *Applied Surface Science*, 556, 145789.

[46] Okorie, O., Buba, A. & Ramalan, A. M. (2017). Optical and dielectric properties of cadmium sulphide thin film grown using chemical bath deposition technique. *IOSR J. of Appl. Phys. (IOSR-JAP)* 5(I), 82-89. www.iosrjournals.org

[47] Desai, H. N., Dhimmar, J. M. & Modi, B. P. (2015). Study of linear and non-linear optical parameters of zinc selenide thin film. *Int. J. Engr. Res. Appl*., 5(6), 117-22.

[48] Okorie, O. & Buba, A. (2023). Studies on the optical dispersion parameters and electronic polarizability of cadmium sulphide thin film. *Asian J. Res. Rev. Phys.*, 7(2), 1-14. https://doi.org/10.9734/ajr2p/2023/v7i2134

[49] Ali, S., Khan, M. & Ahmed, R. (2020). Influence of dopants on the dielectric and optical properties of ZnO thin films. *Journal of Materials Science Research*, 10(3), 45-54.

[50] Timoumi, A., Bouzouita, H. & Rezig, B. (2013). Characterization and Wemple-Didomenico model of indium sulphide thin layers for photovoltaic applications. *Australian Journal of Basic and Applied Sciences*, 7(2), 448-456.

[51] Kumar, R., Singh, M. & Sharma, R. (2019). Optical and dielectric behavior of Co-doped ZnO thin films. *Materials Today: Proceedings*, 25, 156-163.

[52] Dalouji, V. (2018). Influence of surface topography and annealing temperature on the surface and volume of dissipation electrical energy and Spitzer–Fan model in Al doped ZnO films. *Optical and Quantum Electronics*, 50, 325.

[53] Yingrui, S, Yanjie, W., Yu Z., Zhanwu, W., Maobin, W. & Bin, Y. (2017). Indium effect on structural, optical and electrical properties of Cu In_x Zn_{1-X} SnS_4 alloy thin films for solar cell, superlattices and microstructures, doi: 10.1016/j.spmi.2017.07.015.

[54] Usha, K. S., Sivakumar, R. & Sanjeeviraja, C. (2013). Optical constants and dispersion energy parameters of NiO thin films prepared by radio frequency magnetron sputtering technique. *Journal of Applied Physics*, 114, 123501.